

## Removal of 4-Chloro-2-Methoxyphenol from Aqueous Solution by Adsorption to Oil Palm Shell Activated Carbon Activated with $K_2CO_3$

Bakhtiar K. Hamad\*, Ahmad Md. Noor and Afidah A. Rahim

School of Chemical Science, Universiti Sains Malaysia,  
11800 USM Pulau Pinang, Malaysia

\*Corresponding author: bakhtiarkh@yahoo.com

**Abstract:** *Oil palm shell activated carbon (OPSAC) was investigated for adsorption of 4-chloro-2-methoxyphenol (4C2MP) in aqueous solution. The effects of solution pH, agitation time, and initial concentration were evaluated. Adsorption increased as the contact time increased with the highest adsorption obtained in acidic conditions. The Brunauer-Emmett-Teller (BET) surface area was  $1571 \text{ m}^2/\text{g}$ , the total pore volume was  $0.8 \text{ cm}^3/\text{g}$  and the average pore diameter was  $2.15 \text{ nm}$ . Adsorption data were fitted using a Langmuir isotherm, with a maximum monolayer adsorption capacity of  $323.62 \text{ mg/g}$ . Adsorption kinetics were found to follow a pseudo-second-order model.*

**Keywords:** activated carbon, adsorption, 4-chloro-2-methoxyphenol, oil palm shell, potassium carbonate

**Abstrak:** *Karbon teraktif tempurung kelapa sawit (OPSAC) telah dikaji bagi penjerapan 4-kloro-2-metoksifenol (4C2MP) di dalam larutan akues. Penilaian ke atas pengaruh pH larutan, masa pengadukan dan kepekatan awal telah dilakukan. Penjerapan meningkat apabila masa sentuhan meningkat dan penjerapan yang tinggi diperolehi di dalam media berasid. Luas permukaan oleh Brunauer-Emmett-Teller (BET), isipadu liang total dan purata diameter liang adalah masing-masing  $1571 \text{ m}^2/\text{g}$ ,  $0.8 \text{ cm}^3/\text{g}$  dan  $2.15 \text{ nm}$ . Data penjerapan sepadan dengan isoterma Langmuir, dengan kapasiti penjerapan maksimum ekalapisan ialah  $323.62 \text{ mg/g}$ . Kinetik penjerapan didapati mengikuti model tertib-seudo kedua.*

**Kata kunci:** karbon teraktif, penjerapan, 4-kloro-2-metoksifenol, tempurung kelapa sawit, kalium karbonat

### 1. INTRODUCTION

Chlorophenols are one of the most important groups of priority contaminants because they are not readily biodegradable and are highly toxic, causing problems with the human respiratory and nervous system. Many industries, including pesticide, textile, petroleum, pharmaceutical production and paper manufacturing, are sources of chlorophenols in wastewater.<sup>1,2</sup> 4-chloro-2-

methoxyphenol (4C2MP) is a type of chlorophenol found in paper industry wastewater.<sup>3</sup> Chlorophenols are considered to be toxic and carcinogenic by the US Environmental Protection Agency (EPA).<sup>4-6</sup> The maximum concentration of phenol allowed in tap water by the European Union (EU) is  $0.05 \mu\text{gL}^{-1}$ .<sup>1</sup> Thus, removing chlorophenols from aqueous solution is important prior to discharging wastewater into the environment.

A variety of treatments have been used previously to eliminate chlorophenols from aqueous solution, including catalytic wet oxidation, photochemical and biological treatment methods. Adsorption onto activated carbon also shows promising potential as an effective method for removing chlorophenols.<sup>7-10</sup>

Recently, there has been an increasing trend towards the preparation of activated carbon from agricultural by-products as these materials are high quality and inexpensive sources of activated carbon.<sup>11</sup> In Malaysia, a large amount of oil palm shells are generated annually. Previous studies have found that the oil palm shell contains high levels of carbon and low levels of ash, making it a good raw material for preparing activated carbon as an adsorbent. In addition to being economical, this use helps reducing environmental wastage.<sup>12</sup>

In the present study, oil palm shell raw material was used to prepare activated carbon to remove 4C2MP from aqueous solution using potassium carbonate ( $\text{K}_2\text{CO}_3$ ) as the activating agent. The adsorption isotherms, kinetics and thermodynamics of 4C2MP onto oil palm shell activated carbon (OPSAC) were obtained.

## **2. EXPERIMENTAL**

### **2.1 Materials**

A stock solution was prepared by dissolving 1 g of 4C2MP (Sigma Aldrich) in 1 L of distilled water. From this original stock solution, six test solutions with various concentrations (30, 60, 90, 125, 175, and 225 mg/L) were prepared with distilled water.

### **2.2 Preparation of the Activated Carbon**

The oil palm shell was obtained from a palm factory in Nibong Tebal, Penang, Malaysia. Raw material was washed with hot distilled water to remove impurities and dried prior to being cut into small pieces (2–3 mm). The impregnation process was performed by mixing 100 g of raw material with a

43%  $K_2CO_3$  solution at a ratio of 1:2 (w:v). This mixture was heated in a 85–90°C water bath for 24 h. The raw material was then sieved, washed with distilled water until the solution pH reached 7.0 and dried overnight in a 100°C oven. The sample was then placed in a vertical tubular stainless steel reactor and placed in a furnace.

Carbonisation was conducted under high purity (99.99%) nitrogen gas at a flow rate of 150  $cm^{-3}/min$ . The furnace temperature was increased at a rate of 5°C/min to a final temperature of 800°C. The temperature was then held at 800°C for 2 h. The product was cooled to room temperature (30°C), washed with distilled water, and then dried in a 100°C oven. The carbonised material was then activated under  $CO_2$  gas using the same temperature conditions used for carbonisation and held at 800°C for 1.5 h. The product was then washed with distilled water until the solution pH was between 6 and 7 and then dried.

### 2.3 Batch Adsorption Studies

Batch adsorption was studied to determine the removal efficiency of 4C2MP in aqueous solution at a range of initial concentrations (30–225 mg/L). Approximately 0.1 g of OPSAC was added to 250 mL reagent bottles containing 100 ml of a 4C2MP solution. Samples were kept in an isothermal (30°C) water bath and shaken at 140 rpm for 24 h to reach an equilibrium state. Prior to analysis, samples were filtered to separate activated carbon from the adsorbate and minimise interferences. Ultraviolet-Visible (UV-Vis) spectrophotometry (JASCO V-530) was used to determine the concentrations of 4C2MP that remained in solution at 282 nm.

The extent of 4C2MP adsorption at equilibrium,  $q_e$  (mg/g), was calculated using Eq. (1):

$$q_e = \frac{(C_0 - C_e)V}{W} \quad (1)$$

$C_0$  corresponds to the initial concentration of 4C2MP, and  $C_e$  (mg/g) corresponds to the concentration of 4C2MP at equilibrium.  $V$  (L) is the volume of the solution, and  $W$  (g) is the mass of the dry adsorbent.<sup>13</sup> Kinetic studies for the adsorption of 4C2MP were carried out at 30°C with an initial 4C2MP concentration ranging between 30–225 mg/L. The amount of adsorption at time  $t$ ,  $q_t$  (mg/g), was calculated using Eq. (2):<sup>14</sup>

$$q_t = \frac{(C_0 - C_t)V}{W} \quad (2)$$

where  $C_t$  (mg/L) is the adsorbate concentration at time,  $t$  (h). The percentage of 4C2MP removal was calculated using Eq. (3):

$$\text{Removal (\%)} = \frac{(C_0 - C_e)}{C_0} \times 100 \quad (3)$$

The effect of solution pH on 4C2MP removal was studied by varying the pH from 2 to 12 over a period of 5 h. The pH was adjusted by adding either 0.01 M HCl or 0.01 M NaOH. The initial concentration of 4C2MP was 60 mg/L. Parameters other than pH, such as adsorbent dosage, agitation speed, and solution temperature, remained constant.

#### 2.4 Characterisation of Activated Carbon

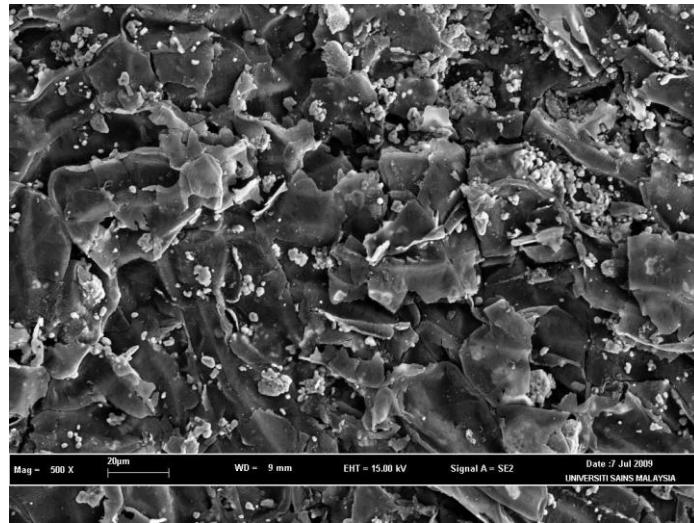
Fourier Transform Infrared (FTIR) analysis (FTIR-2000, Perkin Elmer) was used to detect the available functional groups on the OPSAC surface. Scanning electron microscopy (SEM; Model Leo Supra 50VP Field Emission, Germany) was used to characterise the morphology of the adsorbent surface. The specific surface area, pore volume, and the average pore diameter of the adsorbent were determined using the Brunauer-Emmett-Teller (BET) equation and a Quantachrome Nova Win2© 1994–2002.

### 3. RESULTS AND DISCUSSION

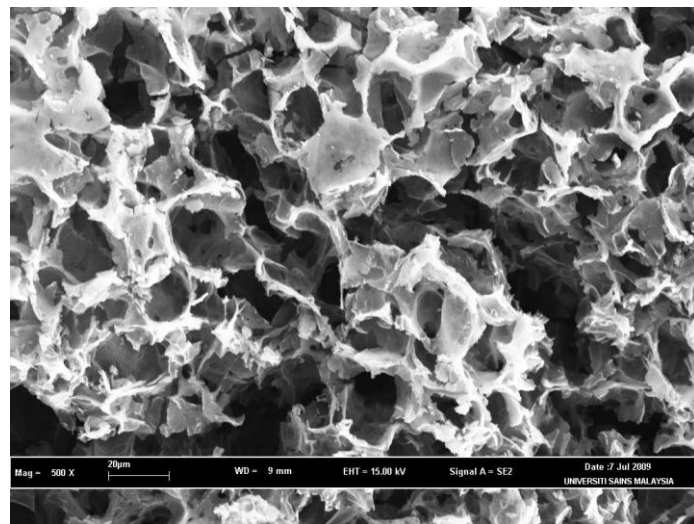
#### 3.1 SEM and BET Tests of Prepared OPSAC

Figure 1(a) shows an SEM micrograph of the surface morphology of the raw material precursor while Figure 1(b) shows the pore size of the OPSAC. The activation process with  $K_2CO_3$  created variable pore sites shown in Figure 1(b). These pores are not present in the raw material as shown in Figure 1(a).<sup>15</sup>

The BET surface area of the prepared OPSAC was  $1571 \text{ m}^2/\text{g}$  and the total volume of pore diameter was  $0.8 \text{ cm}^3/\text{g}$ . The average pore diameter of the activated carbon was 2.15 nm, indicating that the prepared OPSAC was in the mesopore range. Figure 2 illustrates the nitrogen adsorption–desorption isotherms at 77 K for  $K_2CO_3$ -activated OPSAC at  $800^\circ\text{C}$ . The adsorption curve exhibits a hysteresis loop when the relative pressure is increased to 0.4, indicating a mix of Type I (microporous) and Type IV (mesoporous) isotherms.<sup>16,17</sup> The BET and SEM results suggest that 4C2MP will likely adsorb onto OPSAC.



(a)



(b)

Figure 1: SEM micrographs of the oil palm shell (500× magnification) (a) before and (b) after carbonisation at 800°C.

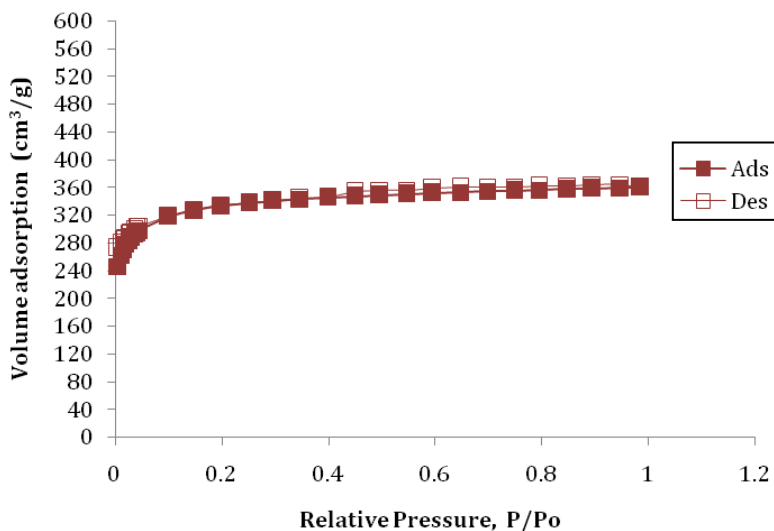


Figure 2: Nitrogen adsorption/desorption isotherms for  $K_2CO_3$ -activated OPSAC.

### 3.2 FTIR of OPSAC Adsorbent

The FTIR spectrum of the OPSAC revealed different functional groups. Figure 3 shows the FTIR adsorption spectrum of the adsorbent. The band at  $3416\text{ cm}^{-1}$  could be attributed to the O-H stretching vibration of hydroxyl functional phenolic groups, including hydrogen bonding due to adsorbed water. The peak at  $1628\text{ cm}^{-1}$  is attributed to conjugated C=O stretching in carboxylic groups and the presence of a quinone structure. The bands at  $1395\text{ cm}^{-1}$  are assigned to C-H bending in alkane or alkyl groups. The broad band between  $1300$  and  $1000\text{ cm}^{-1}$  is due to C-O stretching in alcohols and phenols. The band at  $827\text{ cm}^{-1}$  is attributed to C-OH out-of-plane bending in ether groups.<sup>16-20</sup>

### 3.3 Investigation of Sorption Parameters

#### 3.3.1 Effect of pH

Figure 4 shows that the removal of 4C2MP decreased with increasing pH. This is likely due to the fact that adsorbate ionisation is affected by the pH of the solution. Chlorophenols are proton donors; therefore, they become anionic when the pH of solution is greater than the  $pK_a$  of the chlorophenol ( $pH > pK_a$ ). The  $pK_a$  of 4C2MP is 9.52, thus, adsorption decreases when the pH is greater than 9.52 due to the repulsive forces between the negative groups on the OPSAC surface and phenoxide ions.<sup>1,21</sup> As shown in Figure 4, the highest removal of

4C2MP (84.05%) occurred at pH = 2, while the lowest removal (56.36%) occurred at pH = 12. These values were obtained after a 5 hour time period with a 60 mg/L 4C2MP solution.

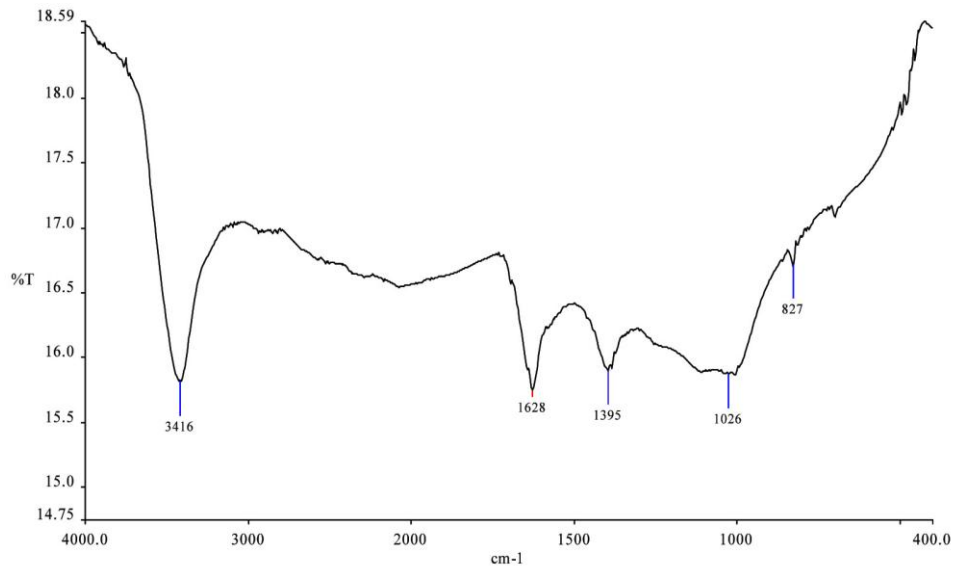


Figure 3: FTIR spectrum of OPSAC.

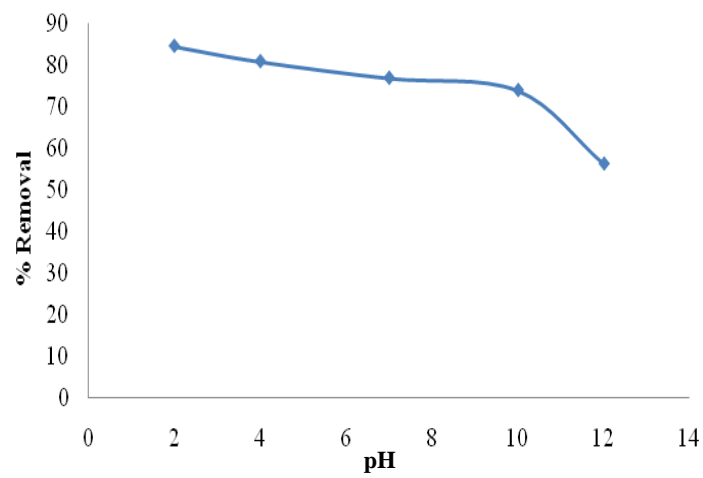


Figure 4: Effect of the varying pH on 4C2MP removal by OPSAC.

### 3.3.2 Effect of contact time and initial concentration on 4C2MP adsorption

Figure 5 shows the effects of contact time and initial concentration on 4C2MP removal by OPSAC. The results showed that, during the first 10 hours, adsorption increased rapidly with increasing concentrations of 4C2MP. At that time, the adsorption reached an equilibrium state. In this study, the adsorption uptake at equilibrium,  $q_e$ , increased from 27.06 to 185.22 mg/g as initial concentration was increased from 30 to 225 mg/L (Table 2). Figure 5 shows that a 10 hour contact time was required to attain adsorption equilibrium for all 4C2MP solutions. During this time more than 82% of the adsorbate was adsorbed due to the initial availability of a large number of pores on the OPSAC surface. Over time, the pore sites became occupied by adsorbate molecules and adsorption decreased.<sup>5</sup>

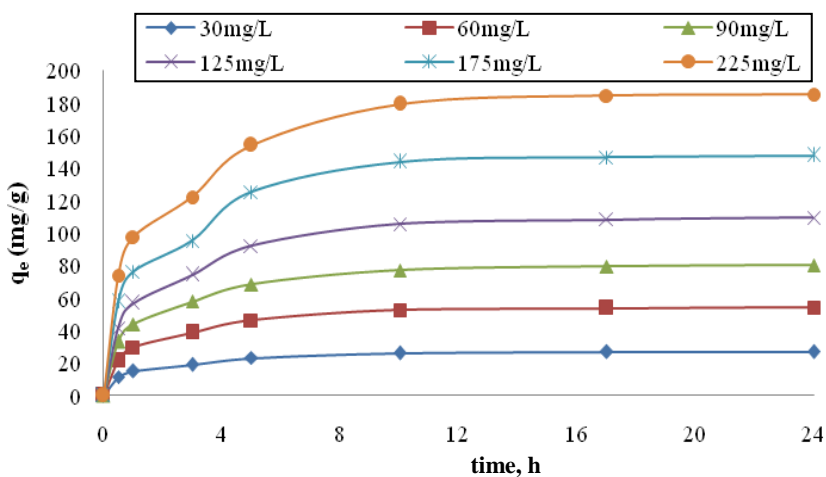


Figure 5: Effect of contact time on the adsorption of various concentrations of 4C2MP onto OPSAC at 30°C.

### 3.4 Adsorption Isotherms

Several models have been used to describe experimental data for adsorption isotherms. However, among these, the Langmuir and Freundlich isotherms are the most appropriate models for this study. According to the Langmuir isotherm, adsorption occurs at homogenous sites and forms a monolayer. In other words, once adsorbate is attached to a site, no further adsorption can take place.<sup>23</sup> The linear form of Langmuir isotherm equation is given as:

$$\frac{C_e}{q_e} = \frac{1}{q_{max}b} + \frac{C_e}{q_{max}} \quad (4)$$

where  $q_e$  (mg/g) is the equilibrium concentration of 4C2MP in the adsorbed phase and  $C_e$  (mg/L) is the equilibrium concentration of 4C2MP in the liquid phase. Langmuir constants, which are related to the sorption capacity ( $q_{max}$ ) and energy of sorption ( $b$ ) can be calculated from the slope of the linear plot of  $C_e/q_e$  vs.  $C_e$ .

Table 1 shows the values of the coefficient correlation ( $R^2$ ),  $q_{max}$  and  $b$  calculated from the plot in Figure 6(a) using the least squares method. The  $R^2$  for the adsorption of 4C2MP is 0.989, indicating favorable adsorption of 4C2MP onto OPSAC using the Langmuir isotherm. The value of  $q_{max}$  was 323.62 mg/g, indicating a very strong monolayer adsorption to the surface. The value of  $b$  was 0.03 L/g, a favorable sorption energy.

The Freundlich isotherm, on the other hand, assumes that adsorption takes place on heterogeneous sites with different distributions of energy levels.<sup>24</sup> The logarithmic equation form of Freundlich isotherm is given in the following equation:

$$\ln q_e = \ln k_f + \frac{1}{n} \ln C_e \quad (5)$$

where  $q_e$  (mg/g) is the equilibrium concentration of 4C2MP in the adsorbed phase and  $C_e$  (mg/L) is the equilibrium concentration of 4C2MP in the liquid phase. The Freundlich constants are related to the sorption capacity ( $K_f$ ) and intensity ( $n$ ). These constants can be calculated from the slope and intercept of the linear plot of  $\ln q_e$  vs.  $\ln C_e$ .

Table 1: Isotherm parameter constants for 4C2MP adsorption onto OPSAC.

Temperature (°C)	Langmuir Isotherm			Freundlich Isotherm		
	$q_{max}$ (mg/g)	$b$	$R^2$	$K_f$	$n$	$R^2$
30	323.62	0.03	0.989	14.02	0.721	0.983

Table 1 also shows the Freundlich parameters calculated from Figure 6(b). The  $K_f$  is 14.02 and the  $n$  is 0.721. The high value of  $K_f$  indicates favorable adsorption conditions for 4C2MP in aqueous solution. The  $R^2$  for the adsorption 4C2MP was 0.983, slightly less than that of Langmuir isotherm and consequently, a less favorable adsorption.

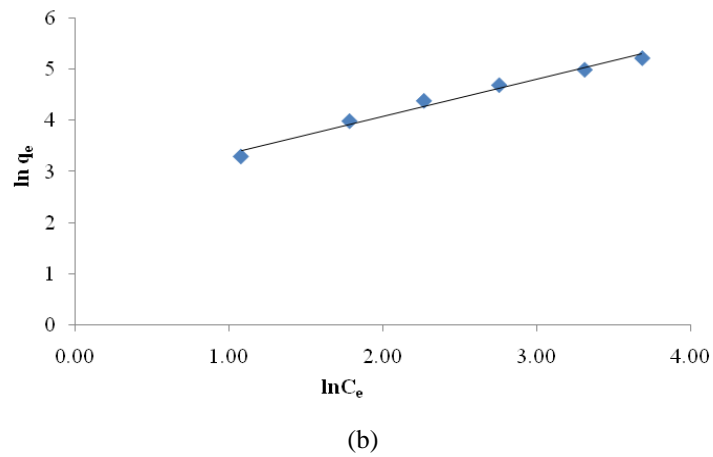
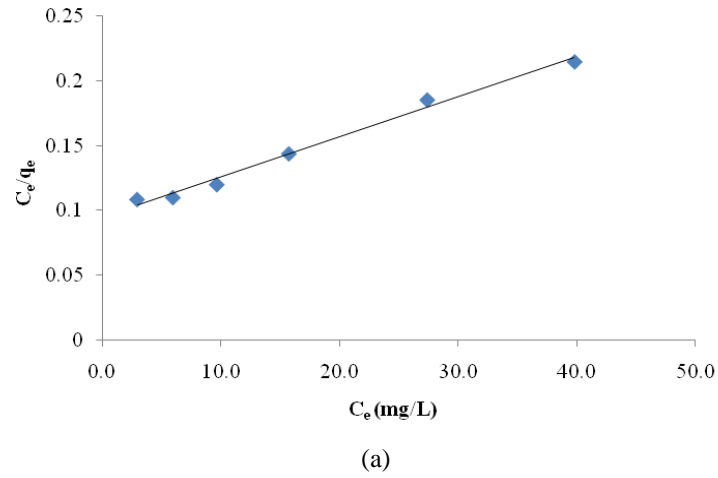


Figure 6: (a) Langmuir and (b) Freundlich isotherms for 4C2MP adsorption onto OPSAC at 30°C.

### 3.5 Kinetic Modeling

To investigate the kinetics of 4C2MP adsorption onto OPSAC, adsorption constants were determined using both pseudo-first order and pseudo-second order models.<sup>25</sup> The pseudo-first order equation is as follows:

$$\log(q_e - q_t) = \log q_e - \frac{k_1}{2.303} t \quad (6)$$

where  $k_1$  ( $\text{min}^{-1}$ ) is the rate constant of the pseudo-first order sorption,  $q_t$  (mg/g) is the amount of sorption at time  $t$  (min), and  $q_e$  (mg/g) is the amount of sorption

at equilibrium. The sorption rate constant,  $k_1$ , can be measured by plotting  $\log(q_e - q_t)$  vs.  $t$ , as shown in Figure 7(a).

The rate constants for the adsorption of 4C2MP onto OPSAC were treated with the Lagergren first-order equation. Table 2 shows the  $R^2$  values and the rate constants for the first-order kinetic model. The rate constants decreased as the concentration increased from 30 to 225 mg/L. The  $R^2$  values for the first-order kinetic model were not high for all adsorbate concentrations. Additionally, these results revealed that there is a relative deviation between calculated and experimental  $q_e$  values indicating that this model does not appropriately describe the adsorption process.<sup>25</sup>

Adsorption kinetics were better explained with the pseudo-second-order model, which can be written as:

$$\frac{t}{q_t} = \frac{1}{k_2 q_e^2} + \frac{1}{q_e} t \quad (7)$$

where  $k_2$  (g/mg·h) is the rate constant.  $k_2$  and  $q_e$  can be obtained from the intercept and slope of plotting  $t/q_t$  vs.  $t$ . Table 2 shows the  $k_2$  values. These values better correspond to the adsorbate concentrations that were calculated from the slopes of the corresponding linear plots of  $t/q_t$  vs. time,  $t$ , shown in Figure 7(b). The rate constants listed in Table 2 generally decreased as the 4C2MP concentrations increased. The  $R^2$  values for all the concentrations of 4C2MP were calculated to be either 0.999 or 0.998. Additionally, there was a strong relationship between the calculated and experimental  $q_e$  values, indicating that the process follows pseudo-second-order kinetics.<sup>25</sup>

Table 2: Pseudo-first-order and second-order rate constants at different initial concentrations of 4C2MP adsorption onto OPSAC at 30°C.

$C_o$ (mg/g)	$q_{e,exp}$ (mg/g)	Pseudo-first-order kinetic model			Pseudo-second-order kinetic model		
		$q_{e,cal}$ (mg/g)	$k_1$ (1/h)	$R^2$	$q_{e,cal}$ (mg/g)	$k_2$ (g/mg h)	$R^2$
30	27.06	19.03	0.126	0.978	26.57	0.035	0.999
60	54.05	42.82	0.130	0.987	58.82	0.017	0.999
90	80.35	65.43	0.127	0.993	79.33	0.013	0.999
125	109.28	87.31	0.124	0.982	105.00	0.007	0.999
175	147.63	122.16	0.126	0.956	146.43	0.005	0.998
225	185.22	154.87	0.115	0.973	196.17	0.004	0.998

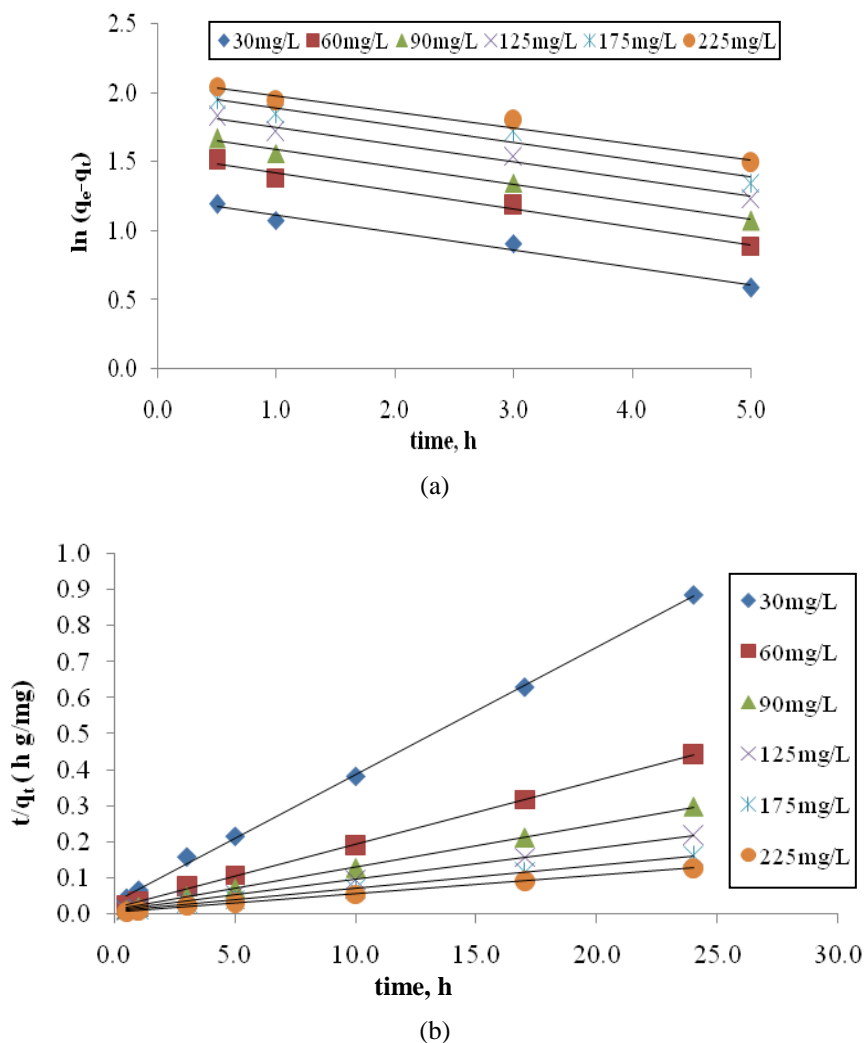


Figure 7: (a) Pseudo-first-order and (b) Pseudo-second-order kinetics for 4C2MP adsorption onto OPSAC at 30°C.

### 3.6 Adsorption Thermodynamics

Adsorption thermodynamics were studied to gain knowledge of adsorption behaviors. Parameters that involve changes in Gibbs free energy ( $\Delta G^\circ$ ), enthalpy ( $\Delta H^\circ$ ) and entropy ( $\Delta S^\circ$ ) were considered according to the following thermodynamic relationship:

$$\ln K_D = \frac{\Delta S^\circ}{R} - \frac{\Delta H^\circ}{RT} \quad (8)$$

where  $K_D$ , the distribution coefficient of the adsorbent, is equal to  $q_e/C_e$ ,  $T$  (K) is the absolute solution temperature, and  $R$  is the universal gas constant (8.314 J/mol K).  $\Delta H^\circ$  can be calculated from the slope and  $\Delta S^\circ$  can be calculated from the intercept of the Van't Hoff plot of  $\ln K_D$  versus  $1/T$  shown in Figure 9.  $\Delta G^\circ$  can then be calculated using the following equation:

$$\Delta G^\circ = \Delta H^\circ - T \Delta S^\circ \quad (9)$$

Table 3 shows the thermodynamic parameters. In all cases,  $\Delta G^\circ$  is negative, indicating that adsorption is spontaneous in nature. Generally,  $\Delta G^\circ$  values range from 0 to  $-20$  kJ/mol for physical adsorption and  $-80$  to  $-400$  kJ/mol for chemical adsorptions.<sup>26</sup> In this study, the  $\Delta G^\circ$  values ranged from  $-0.62$  to  $-3.20$  kJ/mol, indicating that adsorption is mainly physical.  $\Delta H^\circ$  falls between 2.1 and 20.9 for physical adsorptions or between 80 and 200 kJ/mol for chemical adsorptions.<sup>27</sup> In the present study, the  $\Delta H^\circ$  values ranged between  $-3.10$  and  $-6.86$  kJ/mol, indicating that this adsorption is exothermic. A positive  $\Delta S^\circ$  value indicates that the organisation of the adsorbate at the solid/solution interface becomes more random.<sup>28</sup>

Table 3: Thermodynamic parameters for adsorption of 4C2MP on OPSAC at different concentrations.

$C_o$ (mg/L)	$\Delta H^\circ$ (kJ/mol)	$\Delta S^\circ$ (J/mol K)	$\Delta G^\circ$ (kJ/mol)		
			303 K	313 K	323 K
30	-4.96	2.06	-0.62	-0.65	-0.67
60	-6.53	3.22	-0.98	-0.101	-1.04
90	-3.81	5.02	-1.52	-1.57	-1.62
125	-3.74	3.76	-1.14	-1.18	-1.22
175	-3.10	3.73	-1.13	-1.17	-1.20
225	-6.86	9.91	-3.00	-3.10	-1.20

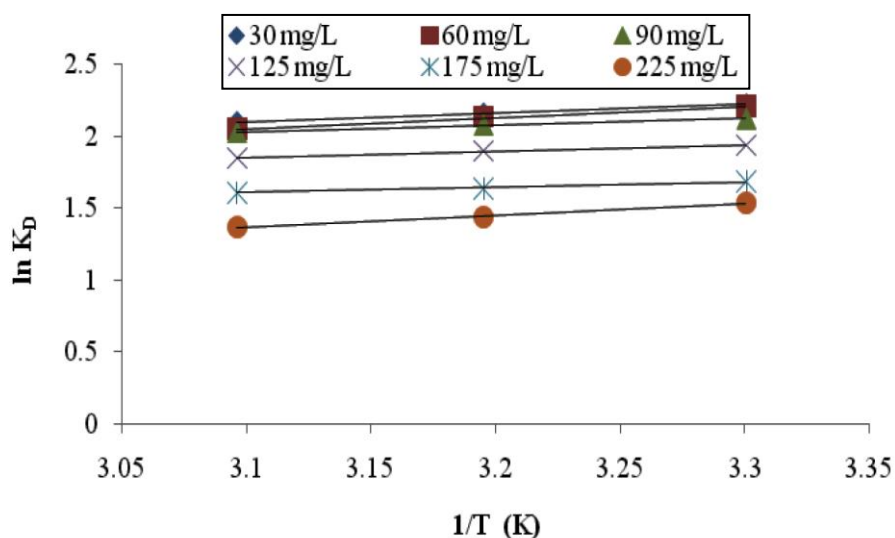


Figure 9: Plot of  $\ln K_D$  versus  $1/T$  at different 4C2MP concentrations.

#### 4. CONCLUSION

$K_2CO_3$  was used as an activation agent to prepare activated carbon from oil palm shell. The resultant oil palm shell activated carbon (OPSAC) was used as an adsorbent to eliminate 4-chloro-2-methoxyphenol (4C2MP) from aqueous solution. The highest removal of 4C2MP was obtained at the lowest pH tested (pH = 2). Removal efficiency also improved with increasing agitation time and decreasing of 4C2MP concentrations. The equilibrium adsorption was best described by the Langmuir isotherm as indicated by high correlation coefficients ( $R^2 = 0.989$ ). Adsorption kinetics followed a pseudo-second-order model with very good correlation coefficients for 4C2MP adsorption. Negative values for  $\Delta G^\circ$  and  $\Delta H^\circ$  indicated that adsorption occurs in a spontaneous and exothermic manner, whereas the positive  $\Delta S^\circ$  values indicated increasing disorder at the solid/solution interface during adsorption. The highest removal of 4C2MP (90.20%) occurred at equilibrium with the 30 mg/L solution.

#### 5. ACKNOWLEDGEMENTS

This research was financially supported by the Research University Grant, Universiti Sains Malaysia (1001/PKIMIA/811007).

## 6. REFERENCES

1. Hamad, B. K., Ahmad, M. N. & Afidah, A. R. (2010). High removal of 4-chloroguaiacol by high surface area of oil palm shell-activated carbon activated with NaOH from aqueous solution. *Desalination*, 257, 1–7.
2. Fattahi, N., Assadi, Y. & Hosaseini, M. R. (2007). Determination of chlorophenols in water sample using simultaneous dispersive liquid-liquid microextraction and derivatization followed by gas chromatography-electron-capture detection. *J. Chromatogr. A*, 1157(1–2), 23–29.
3. Sharma, C., Mohanty, S., Kumar, S. & Rao, N. J. (1999). Gas chromatographic determination of pollutants in kraft bleaching effluent from the Eucalyptus pulp. *Anal. Sci.*, 15, 1115–1121.
4. Calace, N., Nardi, E., Petronio, B. M. & Pietroletti, M. (2002). Adsorption of phenols by paper mill sludges. *Environ. Pollut.*, 118, 315–319.
5. Tan, I. A. W., Ahmad, A. L. & Hameed, B. H. (2009). Adsorption isotherm, kinetics, thermodynamics and desorption studies of 2,4,6-trichlorophenol on oil palm empty fruit bunch-based activated carbon. *J. Hazard. Mater.*, 164, 473–482.
6. Tsutsui, T., Hayashi, N., Maizumi, H. & Huff, J. (1997). Benzene-, catechol-, hydroquinone- and phenol-induced cell transformation, gene mutations, chromosome aberrations, aneuploidy, sister chromatid exchanges and unscheduled DNA synthesis in Syrian hamster embryo cells. *Mutation Research/Fundamental and Molecular Mechanisms of Mutagenesis*, 373, 113–123.
7. Chaliha, S. & Bhattacharyya, K. G. (2008). Catalytic wet oxidation of 2-chlorophenol, 2,4-dichlorophenol and 2,4,6-trichlorophenol in water with Mn(II)-MCM41. *Chem. Eng. J.*, 139, 575–588.
8. Pouloupoulos, S. G., Nikolaki, M., Karampetsos, D. & Philippopoulos, C. J. (2008). Photochemical treatment of 2-chlorophenol in aqueous solution using ultraviolet radiation, hydrogen peroxide and photo-Fenton reaction. *J. Hazard. Mater.*, 153, 582–587.
9. Aksu, Z. & Yener, J. (2001). A comparative adsorption/biosorption study of mono-chlorinated phenols onto various sorbents. *Waste Manage.*, 21, 695–702.
10. Namane, A., A. Mekarzia, K. B., Belhaneche-Benserma, N. & Hellal, A. (2005). Determination of the adsorption capacity of activated carbon made from coffee grounds by chemicals activation with  $ZnCl_2$  and  $H_3PO_4$ . *J. Hazard. Mater.*, 119, 189–194.
11. Guo, J. & Gui, B. (2008). Preparation of activated carbons by utilizing solid wastes from palm oil processing mills. *J. Porous Mater.*, 15, 535–540.

12. Adinata, D., Daud, W. M. A. & Aroua, M. K. (2007). Preparation and characterization of activated carbon from oil palm shell by chemical activation with  $K_2CO_3$ . *Bioresour. Technol.*, 98(1), 145–149.
13. Alam, M. Z., Muyibi, S. A., Mansor, M. F. & Wahid, R. (2007). Activated carbons derived from oil palm empty-fruit bunches: Application to environmental problems. *J. Environ. Sci.*, 19, 103–108.
14. Mohddin, A. T., Hameed, B. H. & Ahmad, A. L. (2009). Batch adsorption of phenol onto physiochemical-activated coconut shell. *J. Hazar. Mater.*, 161, 1522–1529.
15. Hameed, B. H., Tan, I. A. W. & Ahmad, A. L. (2009). Preparation of oil palm empty fruit bunch-based activated carbon for removal of 2,4,6-trichlorophenol: Optimization using response surface methodology. *J. Hazar. Mater.*, 164, 1316–1324.
16. Cuhadaroglu, D. & Uygun, O. A. (2008). Production and characterization of activated carbon from a bituminous coal by chemical activation. *Afr. J. Biotechnol.*, 7(20), 3703–3710.
17. Liou, T. H. (2010). Development of mesoporous structure and high adsorption capacity of biomass-based activated carbon by phosphoric acid and zinc chloride activation. *Chem. Eng. J.*, 158, 129–142.
18. Rao, M. M., Reddy, D. H., P. Venkaswarlu & Seshaiiah, K. (2009). Removal of mercury from aqueous solutions using activated carbon prepared from agricultural by-product/waste. *J. Environ. Manage.*, 90, 634–643.
19. Guo, J. & Lua, A. C. (2003). Surface functional groups on oil-palm-shell adsorption prepared by  $H_3PO_4$  and KOH activation and their effects on adsorptive capacity. *Chem. Eng. Res. Des.*, 81(5), 585–590.
20. Mohan, D., Singh, K. P. & Singh, V. K. (2008). Wastewater treatment using low cost activated carbons driven from agricultural byproducts—A case study. *J. Hazar. Mater.*, 152, 1045–1053.
21. Hameed, B. H., Chin, L. H. & Rengaraj, S. (2008). Adsorption of 4-chlorophenol onto activated carbon prepared from rattan sawdust. *Desalination*, 225, 185–198.
22. Liu, Q., Zheng, T. & Wang, P. (2009). Adsorption isotherm, kinetic and mechanism studies of some substituted phenols on activated carbon fibers. *Chem. Eng. J.*, 157(2–3), 348–356.
23. Hameed, B. H., Tan, I. A. W. & Ahmad, A. L. (2008). Adsorption isotherm, kinetic modeling and mechanism of 2,4,6-trichlorophenol on coconut husk-based activated carbon. *Chem. Eng. J.*, 144, 235–244.
24. Hameed, B. H. & Rahman, A. A. (2008). Removal of phenol from aqueous solution by adsorption onto activated carbon prepared from biomass material. *J. Hazar. Mater.*, 160, 576–581.

25. Amin, N. K. (2008). Removal of reactive dye from aqueous solutions by adsorption onto activated carbons prepared from sugarcane bagasse pith. *Desalination*, 223, 152–161.
26. Yu, Y., Zhuang, Y. Y., Wang, Z. H. & Qiu, M. Q. (2004). Adsorption of water-soluble dyes onto modified resin. *Chemosphere*, 54, 425–430.
27. Liu, Y. (2009). Is the free energy change of adsorption correctly calculated? *J. Chem. Eng. Data*, 54, 1981–1985.
28. Li, Y. H., Di, Z., Ding, J., Wu, D., Luan, Z. & Zhu, Y. (2005). Adsorption thermodynamic, kinetic and desorption studies of  $\text{Pb}^{2+}$  on carbon nanotubes. *Water Res.*, 39, 605–609.